Exciting prospects for solids: Exact-exchange based functionals meet quasiparticle energy calculations

Patrick Rinke[1,2,*], Abdallah Qteish[1,3], Jörg Neugebauer[4], Matthias Scheffler[1,2,5,6],

[1] Fritz-Haber-Institut der Max-Planck-Gesellschaft, Faradayweg 4–6, D-14195 Berlin, Germany
[2] European Theoretical Spectroscopy Facility (ETSF)
[3] Department of Physics, Yarmouk University, 21163-Irbid, Jordan
[4] Max-Planck-Institut für Eisenforschung, Max-Planck-Str. 1, D-40237 Düsseldorf, Germany
[5] Department of Chemistry & Biochemistry and [6] Materials Department University of California Santa Barbara, Santa Barbara, CA, USA

Received XXXX, revised XXXX, accepted XXXX
Published online XXXX

PACS 71.15.Mb,71.15.Qe,71.45.Gm,71.55.Eq,71.55.Gs

* Corresponding author: e-mail rinke@fhi-berlin.mpg.de

Focussing on spectroscopic aspects of semiconductors and insulators we will illustrate how quasiparticle energy calculations in the G_0W_0 approximation can be successfully combined with density-functional theory calculations in the exact-exchange optimised effective potential approach (OEPx) to achieve a first principles description of the electronic structure that overcomes the limitations of local or gradiant corrected DFT functionals (LDA and GGA).

Copyright line will be provided by the publisher

1 Introduction Density functional theory (DFT) has contributed significantly to our present understanding of a wide range of materials and their properties. As quantum-mechanical theory of the density and the total energy it provides an atomistic description from first principles and is, in the local-density or generalized gradient approximation (LDA and GGA), applicable to polyatomic systems containing up to several thousand atoms. However, a combination of three factors limits the applicability of LDA and GGA to a range of important materials and interesting phenomena. They are approximate (jellium-based) exchange-correlation functionals, which suffer from incomplete cancellation of artificial self-interaction and lack the discontinuity of the exchange-correlation potential with respect to the number of electrons. As a consequence the Kohn-Sham (KS) single-particle eigenvalue band gap for semiconductors and insulators underestimates the quasiparticle band gap as measured by the difference of ionisation energy (via photoemission spectroscopy (PES)) and electron affinity (via inverse PES (IPES)). This reduces the predictive power for materials whose band gap is not know from experiment and poses a problem for calculations where the value of the band gap is of importance, e.g. the energies of surface and defect states. Moreover, the incomplete cancellation of the self-interaction questions the applicability to systems with localized defect states, strong magnetic interactions or materials with localized d or f states, such as II-VI compounds, group-III-nitrides, transition metal oxides or lanthanides, actinides and their compounds. It is therefore desirable to have a more advanced electronic structure approach that overcomes these shortcomings of LDA/GGA and provides a reliable description of ground state total energies as well as electronic excitation spectra.

Many-body perturbation theory in the GW approach [1] has developed into the method of choice for describing the energies of electronic excitation spectra of solids (in the following referred to as quasiparticle energies) [2, 3]. For conceptual as well as computational reasons, however, it is currently not feasible to compute total energies for systems of interest. Exact-exchange based DFT functionals on the other hand give access to total energies and thus atomic structures. In addition they largely or in certain

Copyright line will be provided by the publisher

cases completely remove the self-interaction error. Exact-exchange in the optimized effective potential (OEP) approach (OEPx or EXX or OEPx(cLDA) when LDA correlation is added (see also Section 3)) has become the most prominent approach of this kind. It is self-interaction free and greatly improves the comparison of KS eigenvalue differences with quasiparticle excitations for solids, with respect to Hartree-Fock [4–16].

Alternatively, the removal of the self-interaction can be approached by applying the exchange-operator in a non-local fashion within the framework of the generalized Kohn-Sham (GKS) scheme [17] or by using other non-local schemes such as the self-interaction corrected LDA SIC-LDA) method [18]. In the former case the bare exchange interaction is empirically screened and combined with a local potential (commonly referred to as hybrid functional). The most widely used hybrid functionals are PBE0 [19–21], B3LYP [22–24], HSE [25–27] and screened exchange (sX-LDA)[17, 28]. With the exception of SIC and sX-LDA hybrid functionals are only slowly being applied to solids. Almost no experience exist in their combination with GW calculations [29–31] and we will thus defer a discussion of their properties to the outlook.

Combining exact-exchange based DFT calculations with quasiparticle energy calculations [10, 11, 32–34] offers several advantages and will be an important step towards reaching a thorough understanding of the aforementioned systems. Up to now most GW calculations are performed non self-consistently as a single perturbation to an LDA ground state. Unlike the Kohn-Sham scheme in DFT (see Section 3.1) the GW approach in MBPT is not governed by a closed set of equations. Iterating beyond the first order (G_0W_0) in the exact theory would introduce higher order interactions at every step that lead beyond the GW approximation, while iterating the set of GW equations ignoring these contributions generally worsens the good agreement achieved after the first iteration (A more detail account of self-consistency in GW will be given in Section 2.2). From the view point of perturbation theory it would thus be advantageous to use OEPx instead of the LDA[1] as a starting point for G_0W_0 calculations, because the corresponding Kohn-Sham spectrum is closer to the quasiparticle spectrum, thus requiring a smaller correction. This becomes particularly important for materials where LDA severely underestimates the band gap like in ZnO (by ≈80% for the wurtzite phase, LDA (at exp. lattice const.): 0.7 eV, exp: 3.4 eV) or incorrectly predicts a (semi)metallic state as e.g. in germanium (Ge), indium nitride (InN) and scandium nitride (ScN) (see Fig. 1 and 3).

In this Article we will focus only on spectroscopic aspects of semiconductors and insulators and illustrate how quasiparticle energy calculations can be successfully combined with OEPx(cLDA) calculations to achieve a first principles description of the electronic structure that overcomes

[1] All G_0W_0 calculations in this work are performed at the experimental lattice constants.

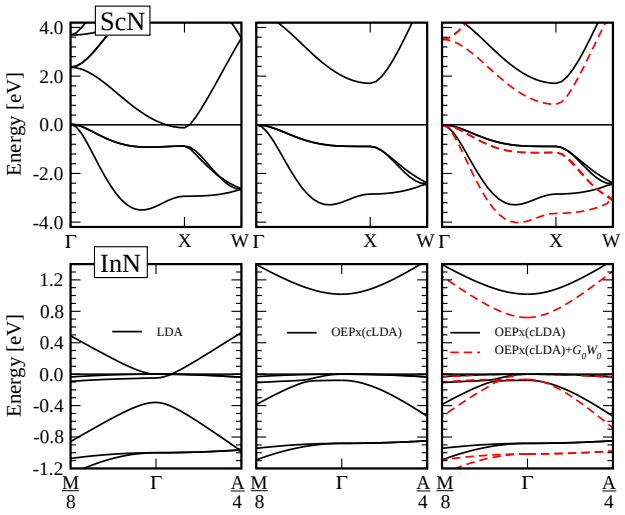

Figure 1 LDA KS calculations incorrectly predict wurtzite InN (bottom) to be a zero-gap semiconductor with the wrong band ordering at the Γ point. ScN (top) is erroneously described as semimetal. In OEPx(cLDA) the band gap opens and InN and ScN correctly become semiconductors, thus providing a more suitable starting point for subsequent quasiparticle energy calculations in the G_0W_0 approximation. All calculations are performed at the experimental lattice constants.

the limitations of LDA and GGA. Figure 1 summarises the structure and the message of this paper. For the example of InN and ScN we demonstrate how OEPx(cLDA) opens the band gap and correctly predicts them to be semiconductors thus providing a better starting point for subsequent G_0W_0 calculations. The quasiparticle corrections to the OEPx(cLDA) band structure are considerable – also for Gallium nitride (GaN) and selected II-VI compounds – bringing the quasiparticle band structure into good agreement with direct and inverse photoemission data. Our OEPx based G_0W_0 calculations have helped to identify the band gap of InN and ScN and to clarify the source for the puzzling, wide interval of experimentally observed band gaps in InN [33, 34].

The article is structured as follows. In Section 2.2 we will briefly review the connection between the single particle Green's function and photo-electron spectroscopy and then introduce the GW method. The exact-exchange approach will be described in Section 3. In Section 4 we will demonstrate why and how the combination of OEPx(cLDA) and GW provides an improved description of the electronic structure. Finally we will conclude in Section 6 and give an outlook in Section 7.

2 Quasiparticle energy calculations

2.1 Photo-electron spectroscopy and the quasiparticle concept In photo-electron spectroscopy (PES) [35–37] electrons are ejected from a sample upon irradiation with visible or ultraviolet light (UPS) or with X-rays

Copyright line will be provided by the publisher

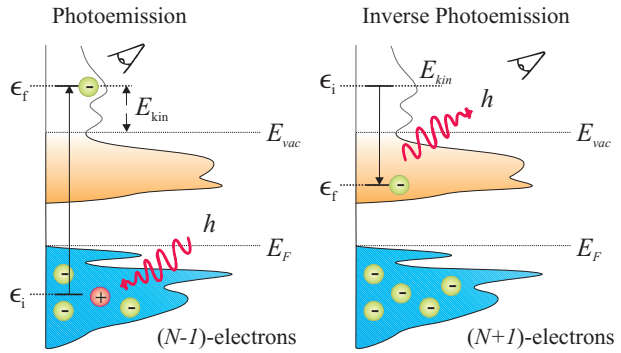

Figure 2 Schematic of the photoemission (PES) and inverse photoemission (IPES) process. In PES (left) an electron is excited by an incoming photon from a previously occupied valence state (lower shaded region) into the continuum (white region, starting above the vacuum level E_{vac}). In IPES (right) an injected electron with kinetic energy $\epsilon_i = E_{kin}$ undergoes a radiative transition into an unoccupied state (upper shaded region) thus emitting a photon in the process.

(XPS), as sketched in the left panel of Fig. 2. Energies $\epsilon_i = h\nu - E_{kin}$ and lifetimes of holes can be reconstructed from the photon energy $h\nu$ and the kinetic energy E_{kin} of the photoelectrons that reach the detector[2]. By inverting the photoemission process, as schematically shown in the right panel of Fig. 2, the unoccupied states can be probed. An incident electron with energy E_{kin} is scattered in the sample emitting *bremsstrahlung*. Eventually it will undergo a radiative transition into a lower-lying unoccupied state, emitting a photon that carries the transition energy $h\nu$. The energy of the final, unoccupied state can be deduced from the measured photon energy according to $\epsilon_f = E_{kin} - h\nu$. This technique is commonly referred to as inverse photoemission spectroscopy (IPES) or bremsstrahlung isochromat spectroscopy (BIS) [38–40].

The experimental observable in photoemission spectroscopy is the photocurrent. Since the energy dependence of the transition matrix elements is usually weak and smooth, structures in the photoemission spectrum can be associated with features in the density of states (DOS), i.e. the imaginary part of the one-particle Green's function[3] [3,41]

$$A(\mathbf{r},\mathbf{r}';\epsilon) = \frac{1}{\pi}\mathrm{Im}\, G(\mathbf{r},\mathbf{r}';\epsilon). \qquad (1)$$

Peaks due to shake ups and shake downs found in XPS are not described by the GW approximation and will therefore not be addressed here.

[2] Throughout this article the top of the valence bands is chosen as energy zero.

[3] The $\mathbf{r}$ and $\mathbf{r}'$ dependence can easily be transformed into a $\mathbf{k}$ dependence. Furthermore only the spin unpolarised situation is discussed here. For the present discussion a summation over the spin indices in the Green's function is therefore assumed.

The Green's function is the solution to the many-body Hamiltonian

$$\hat{H}(\mathbf{r},\mathbf{r}';\epsilon) = \hat{h_0}(\mathbf{r}) + \Sigma(\mathbf{r},\mathbf{r}';\epsilon) \qquad (2)$$

written here in single-particle form where all electron-electron interaction terms are rolled up in the non-local, energy dependent self-energy Σ. The remaining contributions are given by[4] $\hat{h}_0(\mathbf{r}) = -\frac{1}{2}\nabla^2 + v_{ext}(\mathbf{r})$. The external potential v_{ext} is due to the nuclei, after the Born-Oppenheimer approximation of stationary nuclei is taken. The photocurrent is then the surface weighted integral over the diagonal part of the spectral function $A(\mathbf{r},\mathbf{r}';\epsilon)$. We note, however, that with respect to the measured intensities a photoemission spectrum is a noticeably distorted spectral function that in addition is weighted over the momentum components normal to the surface ($\mathbf{k}_\perp$). In particular when selection rules and the energy dependence of the transition matrix elements become important certain peaks in the spectral function may be significantly reduced or may even disappear completely.

The excitation of a non-interacting or a bare particle would give rise to a delta peak in the spectral function. When the electron-electron interaction is turned on, the electrons can no longer be regarded as independent particles. As a consequence the matrix elements of the spectral function $A_{n\mathbf{k}}(\epsilon)$ will contain contributions from many non-vanishing transition amplitudes. If these contributions merge into a clearly identifiable peak that appears to be derived from a single delta-peak broadened by the electron-electron interaction

$$A_{n\mathbf{k}}(\epsilon) \approx \frac{Z_{n\mathbf{k}}}{\epsilon - (\epsilon_{n\mathbf{k}} + i\Gamma_{n\mathbf{k}})} \qquad (3)$$

this structure can be interpreted as single-particle like excitation – the *quasiparticle*[5]. The broadening of the quasiparticle peak in the spectral function is associated with the lifetime $\tau_{n\mathbf{k}} = 2/\Gamma_{n\mathbf{k}}$ of the excitation due to electron-electron scattering, whereas the area underneath the peak is interpreted as the renormalisation $Z_{n\mathbf{k}}$ of the quasiparticle. This renormalisation factor quantifies the reduction in spectral weight due to electron-electron exchange and correlation effects compared to an independent electron.

A computational description of the quasiparticle band structure thus requires the calculation of the Green's function and the self-energy.

2.2 The GW formalism An exact solution to equation (2) is given by Hedin's set of coupled integro-differential

[4] Atomic units $4\pi\epsilon_0 = h = e = m_e = 1$, where e and m_e are the charge and mass of an electron, respectively, will be used in the remainder of this article. If not otherwise stated energies are measured in hartrees and length in bohr.

[5] A *quasielectron* is a new quantum mechanical entity that combines an electron with its surrounding polarisation cloud. The same concept applies to holes.

Copyright line will be provided by the publisher

equations [1]

$$P(1,2) = -i \int G(1,3)G(4,1)\Gamma(3,4,2)d(3,4) \quad (4)$$

$$W(1,2) = v(1,2) + \int v(1,3)P(3,4)W(4,2)d(3,4) \quad (5)$$

$$\Sigma(1,2) = i \int G(1,3)\Gamma(3,2,4)W(4,1)d(3,4) \quad (6)$$

$$\Gamma(1,2,3) = \delta(1,2)\delta(1,3) + \int \frac{\delta\Sigma(1,2)}{\delta G(4,5)} G(4,6)G(7,5)\Gamma(6,7,3)d(4,5,6,7) \quad (7)$$

where the notation $1 \equiv (\mathbf{r}_1, t_1, \sigma_1)$ is used to denote a triple of space, time and spin variables[6]. Accordingly $\int d(1)$ is a shorthand notation for the integration in all three variables of the triple. In eq. 4-7 P is the polarisability, W the screened and v the bare Coulomb interaction and Γ the so called vertex function. By means of Dyson's equation

$$G^{-1}(1,2) = G_0^{-1}(1,2) - \Sigma(1,2), \quad (8)$$

which links the non-interacting system with Green's function G_0 to the fully interacting one (G) via the self-energy Σ, Hedin's equations could in principle be solved self-consistently starting from a given G_0. However, the functional derivative in eq. 7 does not permit a numeric solution, requiring approximations for the vertex function in practise.

Starting from a non-interacting system the initial self-energy is zero and the vertex function becomes $\Gamma(1,2,3) = \delta(1,2)\delta(1,3)$. The first iteration yields Hedin's GW approximation [1] for the self-energy as a function of energy

$$\Sigma_{\mathrm{GW}}(\mathbf{r},\mathbf{r}';\epsilon) = \frac{i}{2\pi}\int_{-\infty}^{\infty} d\epsilon' e^{i\epsilon'\delta} G(\mathbf{r},\mathbf{r}';\epsilon+\epsilon')W(\mathbf{r},\mathbf{r}';\epsilon') \quad (9)$$

where δ is an infinitesimal, positive time. The physical interpretation of the self-energy corresponds to the energy contribution of a particle that arises from the response of the system due to particle's own presence. The interaction of the electrons in the system is mediated by the screened Coulomb interaction rather than the bare one. In the GW formalism W (eq. 5) is calculated in the Random-Phase approximation (i.e. quasiholes and quasielectrons do not interact with each other) from the irreducible polarizability[7] (eq. 4). For the zeroth order Green's function G_0 a Kohn-Sham Green's function G_{KS} (built from Kohn-Sham energies ($\epsilon_{n\mathbf{k}}$) and wavefunctions ($\phi_{n\mathbf{k}}(\mathbf{r})$))

$$G_0(\mathbf{r},\mathbf{r}',\epsilon) = G_{\mathrm{KS}}(\mathbf{r},\mathbf{r}',\epsilon) = \lim_{\delta\to 0^+}\sum_{n\mathbf{k}} \frac{\phi_{n\mathbf{k}}(\mathbf{r})\phi^*_{n\mathbf{k}}(\mathbf{r}')}{\epsilon - (\epsilon_{n\mathbf{k}} + i\delta\,\mathrm{sgn}(E_{\mathrm{F}} - \epsilon_{n\mathbf{k}}))} \quad (10)$$

is typically taken where E_{F} defines the Fermi level.

Keeping Γ fixed (to delta functions) removes the functional derivative from eq. 4-7. These GW equations could then in principle be solved self-consistently via Dyson's equation (8). However this issue is still a matter of debate [42–46]. Unlike in DFT, a self-consistent solution of the full set of Hedin's equations would go beyond the GW approximation and successively introduce higher order electron-electron interactions through the vertex function with every iteration step. Solving the GW equations self-consistently is therefore inconsistent if no higher order electron-electron interactions are included. It was first observed for the homogeneous electron gas [47] that the spectral features broaden with increasing number of iterations in the self-consistency cycle. Similarly, for closed shell atoms the good agreement with experiment for the ionization energy after the first iteration is lost upon iterating the equations to self-consistency [44]. Imposing self-consistency in an approximate fashion [48–50, 46] is not unique and different methods yield different results. Since the controversies regarding self-consistency within GW have not been resolved conclusively, yet, and research into vertex corrections is still in its infancy [51–53] the majority of all GW calculations is performed employing the zeroth order in the self-energy (G_0W_0). This, however, introduces a dependence of the starting Green's function on the self-energy and thus the quasiparticle energies, which can have a noticeable influence, as we will demonstrate in this article.

To obtain the quasiparticle band structure we solve the quasiparticle equation[8]

$$\left[-\frac{\nabla^2}{2} + v_{ext}(\mathbf{r}) + v_H(\mathbf{r})\right]\psi_{n\mathbf{q}}(\mathbf{r}) + \int d\mathbf{r}'\Sigma(\mathbf{r},\mathbf{r}';\epsilon^{qp}_{n\mathbf{q}})\psi_{n\mathbf{q}}(\mathbf{r}') = \epsilon^{qp}_{n\mathbf{q}}\psi_{n\mathbf{q}}(\mathbf{r}) \quad (11)$$

with the GW self-energy ($\Sigma = \Sigma_{\mathrm{GW}}$) by a approximating the quasiparticle wavefunctions ($\psi_{n\mathbf{q}}$) with the Kohn-Sham ones ($\phi_{n\mathbf{q}}$) [54]. The corrections to the Kohn-Sham eigenvalues ($\epsilon_{n\mathbf{q}}$) are then give by

$$\epsilon^{qp}_{n\mathbf{q}} = \epsilon_{n\mathbf{q}} + \langle\phi_{n\mathbf{q}}|\Sigma_{\mathrm{GW}}(\epsilon^{qp}_{n\mathbf{q}}) - v_{xc}|\phi_{n\mathbf{q}}\rangle \quad (12)$$

where $\langle\phi_{n\mathbf{q}}|\,|\phi_{n\mathbf{q}}\rangle$ denotes matrix elements with respect to the wavefunctions $\phi_{n\mathbf{q}}$ of the preceding Kohn-Sham DFT calculation with exchange-correlation potential v_{xc}.

3 Exact-exchange based DFT

[6] Throughout this article we will only consider systems without any explicit spin dependence and will therefore omit the spin index in the following.

[7] With $\Gamma(1,2,3) = \delta(1,2)\delta(1,3)$ eq. 4 reduces to the much simpler form $\chi_0 = -iGG$.

[8] Note that the Hartree potential $v_H(\mathbf{r})$ defined in the next Section has been separated from the self-energy.

Copyright line will be provided by the publisher

3.1 DFT and the Kohn-Sham band structure With regard to quasiparticle band structures Kohn-Sham DFT calculations not only serve as a starting point for G_0W_0 calculations, they are frequently used to interpret quasiparticle spectra due to the similarity of the Kohn-Sham

$$\left[-\frac{\nabla^2}{2} + v_{eff}[n(\mathbf{r})](\mathbf{r})\right]\phi_i(\mathbf{r}) = \epsilon_i\phi_i(\mathbf{r}) \qquad (13)$$

with the quasiparticle equation (11) and because the correction can often be expressed in terms of first-order perturbation theory (eq. 12). To illustrate the difference between the Kohn-Sham and the quasiparticle picture and to lay the foundations for the discussion of the exact-exchange OEP approach we will briefly review the Kohn-Sham DFT scheme.

The central quantities in DFT are the electron density $n(\mathbf{r})$ and the total energy E_{tot}. The latter is a functional of the former and attains its minimum at the exact ground state density, as proven by Hohenberg and Kohn [55]. This formalism was turned into a tractable computational scheme by Kohn and Sham [56], by assuming that the system of interacting particles can be mapped onto a fictitious system of non-interacting particles moving in an effective local potential $v_{eff}(\mathbf{r})$ that reproduce the same density as the many-body problem of interest. The electron density

$$n(\mathbf{r}) = \sum_i^{occ} |\phi_i(\mathbf{r})|^2 \qquad (14)$$

is composed of the occupied Kohn-Sham orbitals $\phi_i(\mathbf{r})$ that are solutions of the Kohn-Sham equation 13.

In analogy to Hartree theory Kohn and Sham divided the total energy into known contributions such as the kinetic energy of the non-interacting particles T_s, the Hartree energy

$$\begin{aligned} E_H[n] &= \frac{1}{2}\int d\mathbf{r}\, n(\mathbf{r})v_H(\mathbf{r}) \qquad (15)\\ &= \frac{1}{2}\sum_{ij}^{occ}\iint d\mathbf{r}\, d\mathbf{r}'\, \frac{\phi_i^*(\mathbf{r})\phi_i(\mathbf{r})\phi_j^*(\mathbf{r}')\phi_j(\mathbf{r}')}{|\mathbf{r}-\mathbf{r}'|} \quad , \end{aligned}$$

the external energy

$$E_{ext}[n] = \int d\mathbf{r}\, n(\mathbf{r})v_{ext}(\mathbf{r}) \quad , \qquad (16)$$

and an unknown remainder. This last term includes all electron-electron interactions beyond the Hartree mean-field and is defined as the exchange-correlation energy

$$E_{xc}[n] = E_{tot}[n] - T_s[n] - E_{ext}[n] - E_H[n] \quad . \qquad (17)$$

Performing the variation with respect to the density then yields the effective potential

$$v_{eff}[n](\mathbf{r}) = v_{ext}(\mathbf{r}) + v_H[n](\mathbf{r}) + v_{xc}[n](\mathbf{r}) \quad , \qquad (18)$$

where each term in the sum is obtained as functional derivative of the corresponding energy expression. Since the exact form of the exchange-correlation functional is unknown[9] suitable approximations have to be found in practice.

3.2 LDA and self-interaction Probably the most popular and efficient approximation for the exchange-correlation energy to-date is the local-density approximation (LDA) [56]

$$E_{xc}^{\mathrm{LDA}}[n] = \int d\mathbf{r}\; n(\mathbf{r})\epsilon_{xc}^{\mathrm{HEG}}(n)\big|_{n=n(\mathbf{r})} \qquad (19)$$

where $\epsilon_{xc}^{\mathrm{HEG}}(n(\mathbf{r}))$ is the exchange-correlation energy density of the homogeneous electron gas (HEG). Whilst the LDA[10] describes even inhomogeneous systems with startling success in many cases, it does so at the expense of a non-physical electron self-interaction. This is introduced by the Hartree term, that contains a spurious interaction of an electron with itself since the sum in eq. 15 includes all occupied states. Although the LDA fulfills the sum rule and thus correctly removes the self-interaction with respect to the particle number, the shape of the exchange-correlation hole is not correct[11]. Applying the definition of Perdew and Zunger [18] the ensuing self-interaction error can be quantified for every state as

$$\delta_i = \frac{1}{2}\iint d\mathbf{r}\, d\mathbf{r}'\, \frac{|\phi_i(\mathbf{r})|^2|\phi_i(\mathbf{r}')|^2}{|\mathbf{r}-\mathbf{r}'|} + E_{xc}[|\phi_i(\mathbf{r})|^2], \quad (20)$$

which follows directly from eq. 14 and 15 for $i = j$. The self-interaction error is largest for localised states and has a tendency to delocalise the electronic wavefunction [32, 59], a point that we will return to later.

Perdew and Zunger proposed to subtract the sum over all self-interaction contributions δ_i for all occupied states from the expression for the total energy in the LDA (or alternatively the spin-dependent LDA) [18]

$$E_{xc}^{\mathrm{SIC-LDA}}[n] = E_{xc}^{\mathrm{LDA}}[n] - \sum_i^{occ}\delta_i \quad . \qquad (21)$$

[9] To be more precise: according to the Hohenberg-Kohn theorem E_{xc} is a unique functional of the density. However, this does not necessarily imply that E_{xc} can be written in a closed mathematical form as functional of the density. Analogous examples are T_e (the kinetic energy of interacting electrons) and T_s. For the latter one may write down a series expansion, but this does not converge properly. Its evaluation therefore requires the detour via the Kohn-Sham formalism. In fact this exact evaluation of T_s is the strongest reason for using the Kohn-Sham scheme. As far as the exact v_{xc} is concerned it can be expressed in terms of the Green's function and the self-energy via the Sham-Schlüter equation in the context of many-body perturbation theory. Alternatively an exact representation of v_{xc} can be obtained in Görling-Levy perturbation theory [57].

[10] The statements made in this subsection apply also to the generalised gradient approximation.

[11] Only the spherical average of the exchange-correlation hole enters in the expression for the total energy [58], which, at least partly, explains the remarkable success of the LDA

Copyright line will be provided by the publisher

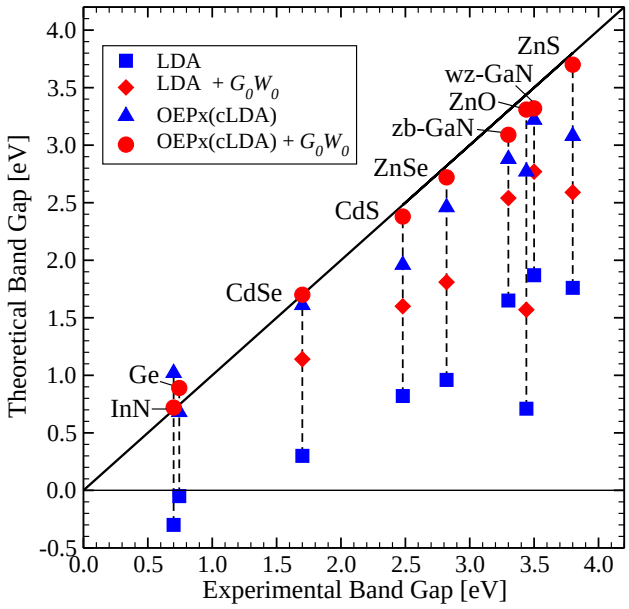

Figure 3 Theoretical versus experimental band gaps: the OEPx(cLDA) based schemes systematically open the band gap compared to the LDA based calculations. Our OEPx(cLDA)+G_0W_0 calculations with the cation d-electrons included as valence electrons agree very well with the experimental values. (For ZnO an estimate of 0.2 eV was added to the zinc-blende values in order to compare to the experimental results for wurtzite.)

The expression for the self-interaction corrected LDA (SIC-LDA) total energy can be minimised according to the variational principle. However, since the energy functional is now orbital dependent, the computational simplicity of the LDA is lost, making SIC-LDA calculations computationally much more demanding than LDA or GGA calculations. Moreover, this form of self-interaction correction vanishes for completely delocalised states, which makes a direct application of this formalism to Bloch states in solids difficult.

It is this self-interaction error in the LDA that is responsible for the fact that InN, ScN and also Ge are incorrectly predicted to be (semi)metals (cf Fig. 1 and Fig. 3) and that the band gap of GaN and II-VI compounds is underestimated severely as shown in Fig. 3. Removing the self-interaction error, as done for instance in the exact-exchange approach, alleviates this problem, despite the fact that the valence and conduction band edge are give by Bloch states, as we will demonstrate in the following.

3.3 The OEP method and exact-exchange Following Kohn and Sham's concept of dividing the total energy into known and unknown contributions the exact-exchange energy E_x

$$E_x = -\frac{1}{2}\sum_{ij}^{occ}\iint d\mathbf{r}\, d\mathbf{r}' \frac{\phi_i^*(\mathbf{r})\phi_j(\mathbf{r})\phi_j^*(\mathbf{r}')\phi_i(\mathbf{r}')}{|\mathbf{r}-\mathbf{r}'|} \quad (22)$$

can be isolated from E_{xc} leaving only the correlation part E_c to be approximated. In the exact-exchange only approach this correlation term is omitted[12] so that the total energy becomes

$$E_{tot}^{\mathrm{x-only}} = T_s + E_{ext} + E_H + E_x \quad . \quad (23)$$

For occupied states the exact-exchange term cancels exactly with the corresponding term in the Hartree potential for $i = j$ and thus removes the self-interaction $\delta_i = 0$ in the Perdew-Zunger sense.

Applying the variational principle to eq. 22 and 23 with respect to the orbitals $\phi_i(\mathbf{r})$ yields the Hartree-Fock approach. Like in the GW approach the eigenenergies and wavefunctions are solutions to a quasiparticle equation – all be it with a hermitian operator

$$\left[-\frac{\nabla^2}{2} + v_{ext}(\mathbf{r}) + v_H(\mathbf{r})\right]\phi_i(\mathbf{r}) + \int d\mathbf{r}'\, \Sigma_x(\mathbf{r},\mathbf{r}')\phi_i(\mathbf{r}') = \epsilon_i\phi_i(\mathbf{r}) \quad . \quad (24)$$

Σ_x is the non-local Fock-operator or exchange self-energy

$$\Sigma_x(\mathbf{r},\mathbf{r}') = -\sum_j^{occ}\frac{\phi_j(\mathbf{r})\phi_j^*(\mathbf{r}')}{|\mathbf{r}-\mathbf{r}'|} \quad . \quad (25)$$

To stay within the framework of density-functional theory the variation of eq. 22 with respect to the density has to be performed instead. This can be done analytically for the exact-exchange energy expression (eq. 22) in the optimised effective potential approach [60–63] and yields the local exchange potential

$$v_x^{\mathrm{OEP}}(\mathbf{r}) = \int d\mathbf{r}' \sum_i^{occ}\sum_j^{unocc} \left[\langle\phi_i|\Sigma_x|\phi_j\rangle\frac{\phi_j(\mathbf{r}')\phi_i(\mathbf{r}')}{\epsilon_i-\epsilon_j} + c.c.\right]\chi_0^{-1}(\mathbf{r}',\mathbf{r}). \quad (26)$$

$\langle\phi_i|\Sigma_x|\phi_j\rangle$ are the matrix elements of the exchange self-energy of eq. 25 and $\chi_0^{-1}(\mathbf{r},\mathbf{r}')$ is the inverse of the static independent particle polarisability

$$\chi_0(\mathbf{r},\mathbf{r}') = \sum_k^{occ}\sum_{n\neq k}^{\infty}\frac{\phi_k^*(\mathbf{r})\phi_n(\mathbf{r})\phi_n^*(\mathbf{r}')\phi_k(\mathbf{r}')}{\epsilon_k-\epsilon_n} + \mathrm{c.c.} \quad . \quad (27)$$

The exchange-potential v_x can be thought of as the best local potential approximating the non-local Fock operator [60]. It is important to emphasise, however, that by construction the total energy in Hartree-Fock is always lower

[12] Later in this section we will reintroduce the correlation energy in an approximate form that is commonly used in connection with exact-exchange DFT calculations.

Copyright line will be provided by the publisher

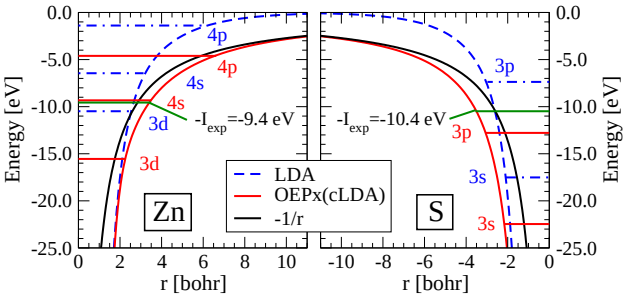

Figure 4 Effective Kohn-Sham potential for the neutral Zn (left panel) and S (right panel) atom: the OEPx(cLDA) potential (red curves) reproduces the correct asymptotic decay $-e^2/r$ (black curves), whereas the LDA (blue, dashed curves) decays exponentially and thus underbinds the electrons. The atomic Kohn-Sham eigenvalues (shown as horizontal lines) are lowered in the OEPx(cLDA) approach compared to the LDA resulting in better agreement with the experimentally measured ionisation potentials (green horizontal lines).

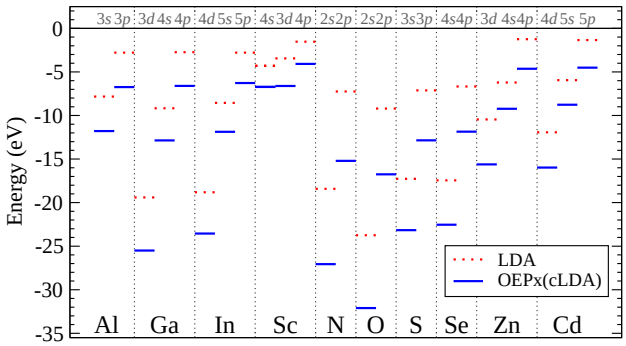

Figure 5 Kohn-Sham eigenenergies of the isolated atoms: The removal of the self-interaction in the OEPx(cLDA) (solid lines) leads to a systematic lowering of all atomic levels compared to the LDA (dotted lines). The downward shift is larger for more localised atomic states, such as the outer valence s and p states in N, O, S and Se.

(or at most equal) and thus better than in the OEPx formalism [64], because the energy minimisation in the optimised effective potential method is subject to the constraint of the wavefunctions being solutions to the Kohn-Sham equation 13. The eigenvalues of the OEPx formalism for the unoccupied states, on the other hand, are closer to the photo-electron excitation energies for the materials presented in this article than the Hartree-Fock single-particle energies. The difference is due to the derivative discontinuity of the exchange potential (see Section 4.2 and 7). In the exchange-only case the discontinuity is particularly large [8, 9, 65, 66], because the conduction band states are poorly accounted for in Hartree-Fock. They are subject to a different potential than the valence states, since the Fock-operator contains the self-interaction correction only for the valence electrons. In OEPx, on the other hand, the Kohn-Sham valence and conduction band states are governed by the same effective potential, which exhibits the correct asymptotic behaviour ($1/r$ decay for large distances in finite systems). The contribution arising from the discontinuity can be calculated separately [17] and when added to the OEPx band gaps the Hartree Fock band gaps are recovered [66].

In OEPx calculations *local* correlation is frequently added by including the LDA correlation energy in the expression of the total energy (eq. 23). Here we follow the parametrization of Perdew and Zunger [18] for the correlation energy density $\epsilon_c^{\rm HEG}[n]$ of the homogeneous electron gas based on the data of Ceperley and Alder [67]. This combination will in the following be denoted OEPx(cLDA).

4 OEPx(cLDA)+G_0W_0

4.1 From the atom to the solid Having established that the removal of the self-interaction in the OEPx(cLDA)-KS approach is the distinguishing feature compared to KS-LDA or KS-GGA calculations we will now illustrate how this leads to an opening of the band gap in solids. For this it is illuminating to start from the eigenvalues of the isolated atoms, depicted in Fig. 4 and 5. The Kohn-Sham potential in OEPx(cLDA) (red curves) is essentially self-interaction free and follows the correct asymptotic $-e^2/r$ potential outside the atom (black curves), whereas the LDA potential (blue, dashed curves) decays exponentially fast. The strong underbinding of the electrons inherent to the LDA is thus greatly reduced in the OEPx(cLDA) approach resulting in a downward shift of all atomic states. The valence electrons of the anion (N, O, S, Se) that take part in the chemical bonding are localised stronger than the respective valence electrons in the cation (Al, Ga, In, Sc, Zn, Cd). The stronger localisation leads to a larger self-interaction correction resulting in a net relative downwards shift of the anion levels with respect to the relevant cation levels (see Fig. 5).

The same behaviour is also observed in SIC-LDA calculations [68] as Tab. 1 demonstrates. In fact for the anions O, S and Se and the 4(5)s in Zn(Cd) Kohn-Sham eigenvalues obtained in the SIC-LDA calculations agree closely with the OEPx(cLDA) ones. The most striking differences are found for the semicore d-electrons, which are significantly lower in SIC-LDA than in OEPx(cLDA). This is due to the fact that the potential in SIC-LDA is non-local. Localising it by means of the optimised effective potential approach denoted here by OEP(SIC-LDA) [69] leads to a significantly narrower spectrum, i.e. the d-electrons (as well as all lower lying states) are moved up in energy. The same behaviour has also been observed for the local/non-local pair of OEPx(cLDA)/Hartree-Fock [71]. The Kohn-Sham energies for both the valence as well as the semicore d-electrons then agree quite well in OEPx(cLDA) and OEP(SIC-LDA).

Taking the example of ScN we demonstrate that the large relative shift of the atomic anion state (N $2p$) also

Copyright line will be provided by the publisher

	Zn		Cd		O		S		Se	
	$4s$	$3d$	$5s$	$4d$	$2p$	$2s$	$3p$	$3s$	$4p$	$4s$
Exp.	-9.4	-17.2	-9.0	-17.6	-13.6	-28.5	-10.4	-20.3	-9.8	-20.2
LDA	-6.2	-10.4	-6.0	-11.9	-9.2	-23.8	-7.1	-17.3	-6.7	-17.5
SIC-LDA	-9.3	-20.0	-8.9	-18.9	-16.5	-31.0	-11.4	-22.4	-10.5	-22.3
OEPx(cLDA)	-9.2	-15.6	-8.8	-16.0	-16.8	-32.1	-12.9	-23.2	-11.9	-22.5
OEP(SIC-LDA)	-9.1	-15.0	-8.4	-15.8	-17.9	-32.8	-12.1	-22.2	-11.1	-21.3

Table 1 Kohn-Sham eigenvalue spectrum of selected isolated atoms. For the valence states SIC-LDA [68], OEPx(cLDA) and OEP calculations for the SIC-LDA functional (OEP(SIC-LDA)) [69] yield very similar energies and improve significantly on the LDA compared to experiment [70] (remaining difference in the two SIC formulations are due to different parametrisation of the LDA functional). For the semicore d-electrons (as well as the lower states not shown here) calculations with a local potential (OEP) give higher eigenvalues than their non-local counterpart.

translates to the solid[13]. In ScN the scandium atom donates its two $4s$ and single $3d$ electron to the nitrogen atom (cf. Fig 6). The five d states of Sc hybridize with the three valence p states of the neighboring N atoms in the rock-salt structure of ScN, forming three p-like bonding, three d-like anti-bonding t_{2g} and two d-like non-bonding e_g bands at the Γ point[14]. The upper three valence bands correspond to the bonding states and originate mainly from the N $2p$ states with some admixture of the Sc $3d$ states, while the lowest conduction band are the anti-bonding t_{2g} states with Sc $3d$ character. The two bands derived from the non-bonding e_g states are more than 1 eV higher in energy [34].

Inspection of the difference between the exchange potential in OEPx(cLDA) ($v_x^{\mathrm{OEPx(cLDA)}}$) and LDA ($v_x^{\mathrm{LDA}}$) shown in Fig. 6(a) reveals that the large relative shift of the atomic anion state (N $2p$) indeed translates to the solid. Fig. 6(a) illustrates that $v_x^{\mathrm{OEPx(cLDA)}}$ is significantly less attractive than v_x^{LDA} in the Sc regions and more attractive around the N atoms. This difference in v_x leads to a significant electron density redistribution (shown in Fig. 6(b)). The electron transfer from the Sc to the N regions gives rise to an increase in the electron negativity difference between the cation and the anion and thus increases the bond polarisation. This in turn, leads to an opening of the band gap – consistent with our OEPx(cLDA) band structure calculations [34].

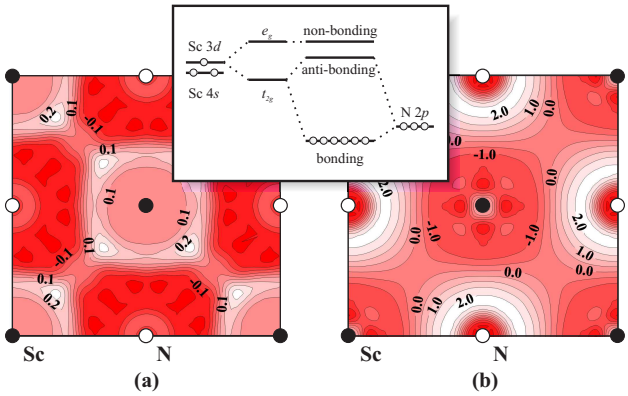

Figure 6 The difference between (a) the OEPx(cLDA) and LDA exchange potentials (in Hartree atomic units) and (b) the valence electron densities (in electrons/unit cell) of ScN (the $1s$ of N and the $1s$, $2s$ and $2p$ of Sc form the core of the pseudopotentials) for one of the square faces of the conventional rock-salt unit cell. Black circles denote Sc and white circles N atoms. The inset shows the bonding scheme together with the electron filling.

In the II-VI compounds and group-III-nitrides this mechanism is also responsible for an opening of the band gap in OEPx(cLDA) compared to LDA, but it is complemented by a contribution arising from the coupling between the anion semicore d-electrons and the $2p$-electrons of the anion. Contrary to ScN the cation d-shell of these compounds is fully filled and the bonding and anti-bonding bands are formed between the $2p$ state of the anion and the highest occupied s states of the respective cation. The bands derived from the d-electrons fall energetically between the anion $2p$ and $2s$ bands. The difference in the partial electron densities plotted along the [111] direction for the example of ZnS and GaN in Fig. 7 reveals that the removal of the self-interaction leads to a localisation of the d-electrons in OEPx(cLDA) compared to LDA. In ZnS, where the d-bands are energetically much closer to the p-derived va-

[13] This was for example realised by Vogl *et al.* who therefore suggested to use SIC-LDA pseudopotentials in regular LDA calculations for the solid [68,72,73]. While this idea is appealing, using a different exchange-correlation functionals for the pseudopotential than for the solid has to be taken with care. In fact LDA calculations performed with OEPx(cLDA) pseudopotentials, that include the d-electrons but not the remaining semicore states in the valence, yield greatly improved d-electron binding energies in GaN and InN, whereas OEPx(cLDA) calculations using the same OEPx(cLDA) pseudopotentials worsens the results again [15].

[14] At other points in the Briouline zone the $4s$ states hybridise, too, which does not change the argument, since the relative shift of the $4s$ and the $3d$ to the N $2p$ level are almost identical.

Copyright line will be provided by the publisher

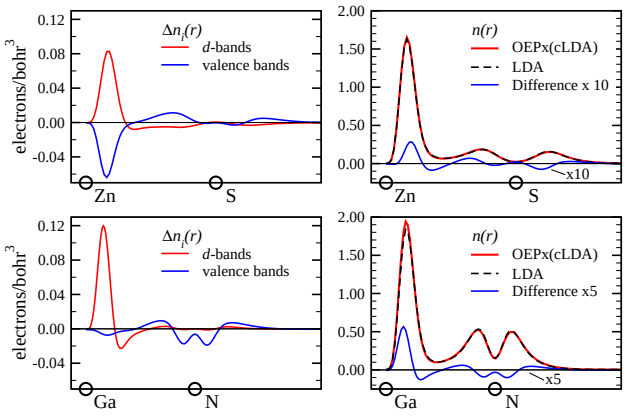

Figure 7 Comparison between OEPx(cLDA) and LDA results for the electron density and the partial densities difference for ZnS (top) and GaN (bottom). Positive density differences indicate an accumulation in OEPx(cLDA). *Left hand side*: partial density differences ($\Delta n_i(\mathbf{r})$) along the [111] direction through the unit cell. The removal of the self-interaction in OEPx(cLDA) leads to a stronger localisation of the d-electrons (red) on the Zn and Ga atoms. In GaN this localisation is not accompanied by a delocalisation of the valence electrons as in ZnS leading to a visible change in the electron density (*Right hand side*: OEPx(cLDA) (red), LDA (black dashed) and their difference (blue line – magnified by a factor of 10 for ZnS and 5 for GaN)).

lence bands than in GaN, the stronger localisation of the d-electrons is accompanied by a delocalisation of the p electrons into the bonding region [32]. The localisation of the d electrons reduces the strength of the pd repulsion and the valence bands are lowered in energy leading to a further opening of the band gap in OEPx(cLDA) [15].

4.2 Discontinuity and the band gap In the Kohn-Sham formalism the system of interacting electrons is mapped onto a fictitious system of non-interacting electrons as alluded to in Section 3. Even in exact DFT only the eigenvalue corresponding to the highest occupied Kohn-Sham state of a finite system can be rigorously assigned to the ionisation potential. For an extended system with well defined chemical potential (Fermi level) this is equivalent to stating that the electron chemical potential in DFT is the same as the true one [56,74–76]. In comparison to quasiparticle energies this leads to an important difference between the Kohn-Sham and the quasiparticle band structure. This is best illustrated for the example of the band gap of semiconductors and insulators. It can be expressed in terms of total energy differences of the N- and $(N \pm 1)$-particle system ($E_{gap} = E(N+1) - 2E(N) + E(N-1)$). Alternatively, the band gap can be entirely formulated in terms of KS eigenvalues as the difference between the electron affinity and the ionisation potential:

$$\begin{aligned} E_{gap} &= \epsilon^{\mathrm{KS}}_{N+1}(N+1) - \epsilon^{\mathrm{KS}}_{N}(N) \qquad (28) \\ &= \underbrace{\epsilon^{\mathrm{KS}}_{N+1}(N+1) - \epsilon^{\mathrm{KS}}_{N+1}(N)}_{\Delta_{xc}} + \underbrace{\epsilon^{\mathrm{KS}}_{N+1}(N) - \epsilon^{\mathrm{KS}}_{N}(N)}_{E^{\mathrm{KS}}_{gap}} \end{aligned}$$

Here $\epsilon^{\mathrm{KS}}_i(N)$ denotes the ith Kohn-Sham state of an N-particle system. E^{KS}_{gap} is the eigenvalue gap of a Kohn-Sham calculation for the N-particle system, given by the difference between the highest occupied and lowest unoccupied state. In a solid, in which $N \gg 1$, the addition of an extra electron only induces an infinitesimal change of the density. Therefore, the two Kohn-Sham potentials must be practically the same inside the solid up to a constant shift and, consequently, the Kohn-Sham wavefunctions do not change. The energy difference Δ_{xc} can then only arise from a spatially constant discontinuity of the exchange-correlation energy upon changing the particle number

$$\Delta_{xc} = \left(\left.\frac{\delta E_{xc}[n]}{\delta n(\mathbf{r})}\right|_{N+1} - \left.\frac{\delta E_{xc}[n]}{\delta n(\mathbf{r})}\right|_{N} \right) + \mathcal{O}\left(\frac{1}{N}\right), \qquad (29)$$

since changes in the Hartree potential will be negligible for $\Delta n(\mathbf{r}) \to 0$ [77–79]. This also implies that the dispersion of bands will not be affected by the discontinuity. The conduction bands will merely be shifted relative to the valence bands.

Whether the (considerable) underestimation of the LDA Kohn-Sham band gaps reported here and elsewhere is a deficiency of the LDA itself or a fundamental property of the Kohn-Sham approach has been a longstanding debate. Similarly it has been argued that the band gaps in the OEPx approach should be larger than the true Kohn-Sham gap, since correlation is omitted [9]. The exchange-correlation energy in the LDA is a continuous function of the density with respect to changes in the particle number and will thus not exhibit a discontinuity even if the band gap were calculated by means of total energy differences. The OEPx formalism, on the other hand, exhibits a derivative discontinuity [80,76], which would be taken into account if the excitation energies were calculated by computing total energy differences between the N and the $N\pm1$ electron system [80]. In KS-DFT, however, this derivative discontinuity does not enter the calculation. The opening of the band gap discussed in Section 4.1 is therefore due to the removal of the self-interaction and not the derivative discontinuity. Adding the corresponding derivative discontinuity would make the band gaps comparable to the Hartree-Fock ones [9,81,65], which are significantly too large.

Further substance to the notion that even the exact Kohn-Sham potential would give rise to a band gap underestimation was first given by Gunnarsson and Schönhammer [82, 83] and Godby *et al.* [79,84] and recently by Grüning *et al.* [81]. Gunnarsson and Schönhammer derive their conclusions from an exactly solvable, Hubbard-like model, whereas

Copyright line will be provided by the publisher

Godby *et al.* and Grüning *et al.* use the Sham-Schlüter formalism to generate the local exchange-correlation potential that corresponds to the G_0W_0 self-energy. They show that the resulting potential closely resembles that of the LDA. Also the Kohn-Sham eigenvalue differences are very similar to the LDA ones, whereas G_0W_0 calculations, that incorporate information of the $(N \pm 1)$-particle system in a natural way (see Section 2), generally give quasiparticle band gaps to within 0.1-0.2 eV of the experimental values [2].

The good agreement of the OEPx(cLDA) band gaps with experiment reported previously [7–13] can therefore be regarded as fortuitous. In fact inspection of Fig. 3 shows that the OEPx(cLDA) band gaps are lower than the experimental ones [32] and hence lower than those of previous studies. This is due to the fact, that unlike in the earlier work we have explicitly included the d-electrons as valence electrons in our pseudopotential calculations. The pd repulsion pushes the valence bands up in energy and shrinks the gap [15]. All-electron OEPx calculations for CdS and ZnS, on the other hand, report band gaps considerably higher than the experimental ones [65]. The origin of this discrepancy between pseudopotential and all-electron calculations is still under debate. A band gap underestimation in OEPx has also been observed for noble gas solids and insulators [14, 65, 66].

Table 2 illustrates for four representative compounds that adding LDA correlation to the OEPx approach has a marginal effect on the calculated band gaps (and the band structure in general – not shown). ZnO is the only material of those studied here where the difference exceeds 0.1 eV. The remaining difference between OEPx(cLDA) and experiment is recovered to a large degree in the G_0W_0 quasiparticle energy calculations as Tab. 2 and Fig. 3 demonstrate.

The advantage of the OEPx(cLDA)+G_0W_0 approach is that it proves to be sufficient to include the d-electrons of the cation explicitly as valence electrons in the pseudopotential without having to include the remaining electrons of the semicore shell, provided OEPx(cLDA) pseudopotentials [97] are used. Taking GaN as an example the $3s$-electrons in the Gallium atom are approximately 130 eV and the $3p$-electrons approximately 80 eV lower than the $3d$ states. Resolving these more strongly localized $3s$ and $3p$-electrons in GaN with a plane-wave basis set will hence require significantly higher plane-wave cutoffs than the 70 Ry required for the d-electrons [32]. In a pseudopotential framework it would thus make sense to explicitly include the d-electrons of the cations in the II-VI compounds and group-III-nitrides as valence electrons, but to freeze the chemically inert semicore s and p-electrons in the core of the pseudopotential. However, due to the large spatial overlap of the atomic semicore s and p with the d wavefunctions, core-valence exchange-correlation is large in these compounds. As a consequence core-valence exchange-correlation is treated inconsistently when going from LDA to LDA+G_0W_0, if pseudopotentials are used in this fashion, because the exchange-correlation self-energy in the GW approach acts on the d-electrons in the solid, but cannot act on the s and p-electrons in the semicore shell, too. The result is a severe underestimation of the LDA+G_0W_0 band gaps (cf. red diamonds in Fig. 3) and d-bands that are pushed energetically into the p-derived valence bands in the II-VI compounds [32, 91, 92] (cf. Tab. 3). The only way to remedy this problem within LDA+G_0W_0 is to free the electrons in question by performing all-electron G_0W_0 calculations [94] or by using pseudopotentials that include the entire shell as valence electrons [91, 92, 48], which in the latter case introduces formidably high plane-wave cutoffs. If, on the other hand, OEPx or OEPx(cLDA) is used for the ground state calculation, then the exchange self-energy already acts on the semicore s and p states in the generation of the pseudopotential. Since the exchange self-energy can be linearly decomposed into a core and a valence contribution no non-linear core corrections [98] arise in the Hartree-Fock case and they are expected to be small for OEPx(cLDA) pseudopotentials [9]. When going from OEPx(cLDA) to OEPx(cLDA)+G_0W_0 core-valence exchange is therefore treated consistently, even when the semicore s and p-electrons are frozen in the core, as long as OEPx(cLDA) pseudopotentials are used [32].

For InN the LDA starting point is so problematic (cf. Fig. 1), that even subsequent all-electron G_0W_0 calculations only open the gap to 0.02 - 0.05 eV [94, 99]. Here the importance of removing the self-interaction from the ground state calculation has been demonstrated before by combining SIC-LDA calculations with G_0W_0 calculations (all be it in a rather approximate way by adjusting the pd repulsion and combining calculations with and without the $4d$-electrons in the core of the In pseudopotential) [100, 101]. The OEPx(cLDA) approach, on the other hand, predicts InN to be a semiconductor, as Fig. 1 illustrates, and G_0W_0 calculations can be applied without further approximations. The size of the band gap of InN and the origins for the considerable spread in the experimental data has been a matter of intense debate over the last years. For wurtzite InN our value of 0.7 eV [33] strongly supports recent experimental findings [102–104]. The OEPx(cLDA)+G_0W_0 calculations have further helped to clarify the source for wide interval of experimentally observed band gaps [33].

For ScN, an emerging versatile material for promising technological applications, the electronic band structure has also been difficult to access experimentally, due to growth related problems. Similar to the metallic state in InN the strong self-interaction effects in the LDA predict ScN to be semimetallic (cf. Fig. 1) preventing a direct application of the LDA+G_0W_0 approach. By using OEPx(cLDA) the ground state becomes essentially self-interaction free. This leads to an opening of the band gap and a suitable semiconducting starting point for G_0W_0 calculations [34], as described in Section 4.1. The OEPx(cLDA)+G_0W_0 calculations lower the OEPx(cLDA) band gap of 1.7 eV

Copyright line will be provided by the publisher

DFT	PP	Conf.	GW	ZnO	ZnS	CdS	GaN
OEPx	OEPx	d		2.34	2.94	1.84	2.76
OEPx(cLDA)	OEPx(cLDA)	d		2.57	3.08	1.96	2.88
OEPx	OEPx	d	GW	3.07	3.62	2.36	3.09
OEPx(cLDA)	OEPx(cLDA)	d	GW	3.11	3.70	2.39	3.09
Experiment				(3.44)	3.80	2.48	3.30
LDA	LDA	no d's	GW		3.98^a	2.83^a	3.10^b
OEPx(cLDA)	OEPx(cLDA)	no d's			3.74^c		3.46^d
OEPx(cLDA)	OEPx(cLDA)	no d's	GW				3.49^e
LDA	LDA	d	GW			1.50^f	
LDA	LDA	d-shell	GW		3.64^g		
LDA	LDA	d-shell	GW		3.50^h	2.45^h	2.88^h
LDA	LDA	d-shell	GW		3.38^i	2.11^i	
LDA	FP	all e^-	GW	$(2.44)^j$	3.24^k		$(3.03)^k$
LDA	ASA	all e^-	GW	$(4.06)^m$	3.97^l		$(3.25)^m$

Table 2 DFT and quasiparticle band gaps in eV for ZnO, ZnS, CdS, and GaN in the zinc-blende structure sorted in increasing energy from top to the experimental values. The first column lists the DFT scheme and the second column denoted PP the pseudopotential used. For all-electron calculations this column denotes if the atomic sphere approximation (ASA) or the full potential (FP) was employed. "Conf." refers to the configurations of the (pseudo)atoms: d-electrons included (d), as described in the previous section, valence only (no d's), d-electrons and their respective shell included (d-shell) and all-electron (all e^-). Experimental results are taken from: ZnO [85], ZnS [86], CdS [87], GaN [88] and the OEPx(cLDA) and GW data from: ^{a}Ref. [89], ^{b}Ref. [90], ^{c}Ref. [13], ^{d}Ref. [8], ^{e}Ref. [10], ^{f}Ref. [91], ^{g}Ref. [48], ^{h}Ref. [92], ^{i}Ref. [49] ^{j}Ref. [93], ^{k}Ref. [94], ^{l}Ref. [95], ^{m}Ref. [96]. Numbers in round brackets refer to wurtzite structures. In Ref. with superscript ^{a} and ^{b} a model dielectric function was employed and in ^{e,f,g,h} a plasmon pole model was used.

down to 0.8 eV [34], clearly supporting recent experimental findings of an indirect gap of 0.9±0.1 eV [105].

While LDA based G_0W_0 calculations generally open the band gap from the underestimated LDA value, we observe here that the G_0W_0 corrections lower the respective gaps of InN and ScN obtained in the OEPx(cLDA) approach. Since G_0W_0 falls into the realm of perturbation theory (cf. eq. 12) this is not unusual, because it is not *a priori* clear if the quasiparticle corrections are positive or negative.

4.3 *d*-electron binding energies A known problem for the group-III-nitrides and the II-VI compounds is, that both KS-LDA and LDA based G_0W_0 calculations underestimate the binding of the d-bands – regardless of whether applied in a pseudopotential or an all-electron fashion. For four selected compounds the center of the d-bands[15] is listed in Tab. 3 for the different computational schemes. For ZnS and CdS OEPx(cLDA) and OEPx(cLDA)+G_0W_0 produce essentially the same d-electron binding energies. Only in ZnO quasiparticle corrections are found to lower the d-states by 1.5 eV compared to OEPx(cLDA), further reducing the pd coupling. Again, adding LDA correlation to the OEPx has essentially no effect on the energies of the bands (energy differences < 0.2 eV).

At first sight it appears surprising that the removal of the self-interaction does not automatically lower the position of the d-bands in OEPx(cLDA). Closer inspection of the atomic eigenvalues in Fig. 5 reveals, however, that the cation d states are shifted down by almost the same amount as the anion p states. The relative position to the p states, from which the top of the valence band is derived, therefore remains similar in OEPx(cLDA) and LDA [15]. Applying exact-exchange in a non-local fashion (Hartree-Fock) instead lowers the d-states considerably [30]. The narrower spectrum of the local exchange potential therefore results in d electron binding energies that are lower in OEPx(cLDA) than in HF. This difference between the local and the non-local incarnation of an exchange-correlation potential pertaining to the same total energy functional is identical to that alluded to previously for the case of isolated atoms in Section 4.1. Core-valence exchange-correlation effects beyond those included via the pseudopotential are thus not expected to change this conclusion.

A recent all-electron OEPx study (line 20) has reported values for ZnS and CdS in better agreement with experiment [65]. However, it is not clear at the present stage, why for CdS the difference to our pseudopotential calcula-

[15] This has been obtained by averaging over the d-bands at the Γ-point.

Copyright line will be provided by the publisher

	DFT	PP	Conf.	GW	ZnO	ZnS	CdS	GaN
1	LDA	LDA	d	GW	4.29	4.30	6.17	13.05
2	OEPx(cLDA)	LDA	d	GW	4.98	5.02	6.40	13.58
3	OEPx(cLDA)	LDA	d		4.36	5.33	6.54	12.75
4	LDA	LDA	d		5.20	6.32	7.72	14.25
5	OEPx	OEPx	d		5.12	6.91	7.57	14.85
6	OEPx(cLDA)	OEPx(cLDA)	d		5.20	7.05	7.61	15.02
7	OEPx	OEPx	d	GW	6.68	6.97	7.66	16.12
8	OEPx(cLDA)	OEPx(cLDA)	d	GW	6.87	7.08	7.75	16.15
9	Experiment				$(9.00)^a$	8.97^a	9.20^b	17.70^c
						9.03^d	9.50^d	
10	LDA	LDA	d	GW			5.20^e	
11	LDA	LDA	d-shell	GW		7.40^f		
12	LDA	LDA	d-shell	GW		6.40^g	8.10^g	15.70^g
13	LDA	LDA	d-shell	GW		6.87^h	8.15^h	
14	LDA	LDA	d-shell	SAT		7.90^g	9.10^i	17.30^g
15	LDA	LDA	d-shell	$G'W'\Gamma$		8.02^h	8.99^h	
16	LDA+U	LDA				8.78^j		
17	LDA+U	LDA	d-shell	GW		7.10^j		
18	LDA	FP	all e^-	GW	6.16^k	7.10^l	8.20^l	$(16.40)^l$
19	LDA	ASA	all e^-	GW	$(5.94)^m$	8.33^n		$(17.60)^m$
20	OEPx	FP	all e^-			9.1^o	8.2^o	

Table 3 d-electron binding energies referenced to the top of the valence band: The layout is the same as in Table 2. Experimental values taken from: ^{a}Ref. [106], ^{b}Ref. [107] ^{c}Ref. [108], ^{d}Ref. [109], and the GW data from: ^{e}Ref. [91], ^{f}Ref. [48], ^{g}Ref. [92], ^{h}Ref. [49] ^{i}Ref. [110], ^{j}Ref. [111] (U=8 eV, J=1 eV), ^{k}Ref. [93], ^{l}Ref. [94], ^{m}Ref. [96], ^{n}Ref. [95]. ^{o}Ref. [65]. SAT denotes GW calculations including plasmon satellites, $G'W'\Gamma$ calculations performed with eigenvalue self-consistency and addition of a vertex contribution. Numbers in round brackets refer to wurtzite structures. In Ref. denoted by ^{d,e,f} a plasmon pole model was used.

tions (line 5) is merely 0.6 eV, whereas for ZnS it amounts to 2.2 eV. It is also not clear if the discrepancy is caused by core-valence linearisation in the pseudopotentials, the use of pseudo- rather than all-electron wavefunctions in the Fock-operator or if it has an entirely different origin.

Overall the binding energies obtained with our OEPx(cLDA)+G_0W_0 approach agree well with other available GW calculations (line 11, 12, 13 and 18 in Tab. 3), but are still about 2 eV at variance with experiment. The reason for this could be twofold. Either interactions beyond the GW approximation are required for describing the excitation of these semicore d-electrons and/or one needs to go beyond even OEPx(cLDA) as a starting point. Evidence that both self-consistency in the GW calculations as well as the inclusion of vertex effects (see Section 2.2) introduce changes in the right direction was recently given by Fleszar and Hanke. Starting from an LDA ground state only eigenvalues (and not also the wavefunction) were iterated to self-consistency in the GW calculations. This increases the binding energy by 0.4-0.5 eV in ZnS and CdS [49]. Adding a vertex function that makes the calculation "consistent" with the LDA starting point[16] increases the binding energy by additional 0.4-0.5 eV (line 15) [49]. Similar conclusions were drawn from a recent study, in which G_0W_0 calculations were based on LDA+U ground states [111]. With increasing U the binding energy of the d-state increases linearly in the LDA+U calculations (line 16) as the pd hybridisation reduces. The G_0W_0 calculations, however, prove to be insensitive to this change and shift the d-bands up again, close to their LDA+G_0W_0 positions (line 17) [111]. Previously Rohlfing *et al.* had devised a way to go beyond the GW approximation by including plasmon satellites in the Green's function, denoted here by SAT (line 14 in Tab. 3). Although the SAT improves on the d-electron binding energies it considerably over-corrects the band gap and the valence part of the band structure [110]. Work towards a consistent description of excitation energies of the semi-

[16] Strictly spoken Σ is only zero on the first iteration when starting from Hartree theory (see Section 2.2). Starting from a Kohn-Sham calculations implies that $\Sigma = v_{xc}$ in which case the vertex function is not given by delta functions, but can still be analytically derived [51].

Copyright line will be provided by the publisher

core d-electrons in these materials is clearly required in the future.

5 Comments on self-sonsistency As alluded to in Section 2.2 it is still a matter of debate how to perform self-consistent GW calculations for quasiparticle band structures. For the non self-consistent G_0W_0 scheme our calculations for the selected II-VI compounds and GaN have revealed a significant dependence on the starting point, if the semicore d-electrons, but not the remaining electrons of the semicore shell, are explicitly taken into account in the pseudopotential calculation. Since for the reasons given in Section 4.2 no meaningful comparison can be made between LDA+G_0W_0 and OEPx(cLDA)+G_0W_0 calculations unless the entire semicore shell is included in the calculation these systems are not suitable to assess the influence of the starting point on the quasiparticle band structure. In ScN, on the other hand, the semicore d-shell of Sc is not fully filled and the remaining s and p-electrons in the semicore shell are much higher in energy. Taking GaN as an example the $3s$-electrons in the Scandium atom are approximately 100 eV and the $3p$-electrons approximately 60 eV higher than in Gallium. Resolving the $3s$ and $3p$-derived bands in ScN with plane-waves thus only requires a cutoff of 80 Ry [34] and makes ScN an ideal candidate for constructing a comparison between LDA+G_0W_0 and OEPx(cLDA)+G_0W_0 calculations.

However, the *negative* LDA band gap (see Table 4) impedes the direct application of the LDA+G_0W_0 formalism with our GW code, since in its current implementation [112–114] a clear separation between conduction and valence bands is required. Therefore, an indirect approach is adopted. First, LDA+G_0W_0 calculations are performed at a lattice constant (a_0 = 4.75 Å) larger than the experimental one (a_0 = 4.50 Å), where the fundamental band gap in the LDA is small but positive. We then use the LDA *volume* deformation potentials (which agrees well with the OEPx(cLDA)+G_0W_0 one) to determine the corresponding LDA+G_0W_0 band gaps at the equilibrium lattice constant[17].

We find (Tab. 4) that the LDA+G_0W_0 and OEPx(cLDA)+G_0W_0 calculations, starting from the two extremes (negative band gap in LDA, 0.8 eV overestimation in OEPx(cLDA)), yield quasiparticle band gaps that agree to within 0.3 eV. Since the LDA-based calculations are close to the limit of metallic screening, whereas the OEPx(cLDA)-based calculations form the opposite extreme of starting from a completely self-interaction free exchange-correlation functional, we expect the results of a self-consistent GW calculation to fall in the range between the LDA+G_0W_0 and OEPx(cLDA)+G_0W_0 calculations. From these results we estimate the maximum error bar associated with omitting self-consistency in GW to be the difference from the arithmetic averages for $E_g^{\Gamma-\Gamma}$, $E_g^{\Gamma-X}$ and E_g^{X-X} (reported in Tab. 4) to the largest deviation between LDA+G_0W_0 and OEPx(cLDA)+G_0W_0, i.e. of the order of 0.15 eV for ScN [34].

[17] This approach is in principle not limited to band gaps and can equally well be applied to the full band structure for example.

Approach	$E_g^{\Gamma-\Gamma}$	$E_g^{\Gamma-X}$	E_g^{X-X}
OEPx(cLDA)+G_0W_0	3.51	0.84	1.98
LDA+G_0W_0	3.71	1.14	2.06
$[G_0W_0]_{\mathrm{average}}$	3.62	0.99	2.02
OEPx(cLDA)	4.53	1.70	2.59
GGA	2.43	−0.03	0.87
LDA	2.34	−0.15	0.75
Experiment			
Ref. [12]	∼3.8	1.30	2.40
Ref. [105]		0.9±0.1	2.15

Table 4 Calculated and experimental band gaps (E_g) of ScN (in eV). $[G_0W_0]_{\mathrm{average}}$ denotes the arithmetic average between the OEPx(cLDA)+G_0W_0 and LDA+G_0W_0 results (see text).

6 Conclusions We have presented the combination of quasiparticle energy calculations in the G_0W_0 approximation with DFT calculations in the OEPx(cLDA) approach. Using OEPx(cLDA) instead of LDA or GGA removes the inherent self-interaction of the latter from the ground state calculation. Starting from the individual atoms we have illustrated how this leads to an opening of the Kohn-Sham band gap in the solid. In the spirit of perturbation theory OEPx(cLDA) thus provides a more suitable starting point for G_0W_0 calculations than LDA or GGA. For materials for which LDA erroneously predict a (semi)-metallic state, like e.g. InN or ScN, OEPx(cLDA) yields a semiconducting ground state, which unlike in the LDA case, permits a direct application of the G_0W_0 approximation. For the II-VI compounds and group-III-nitrides presented here as an example the band gaps in the OEPx(cLDA)+G_0W_0 approach are in excellent agreement with experiment and the position of the semicore d-electron bands no worse than in previous LDA+G_0W_0 calculations.

7 Outlook A disadvantage of the OEPx approach is that it yields total energies and thus structural properties comparable to Hartree-Fock. For the materials considered here all lattice parameters are know from experiment, but this might not be the case for surfaces, defects, nanostructures or new materials. Then, in cases where LDA and GGA are known to fail, exchange-correlation functionals that appropriately include exact-exchange are needed.

In the most pragmatic approach a portion of Hartree-Fock exchange is mixed with a different portion of local

Copyright line will be provided by the publisher

exchange and correlation[18]

$$E_{xc}^{hyb} = E_{xc}^{\mathrm{DFT}} + \alpha(E_x^{\mathrm{HF}} - E_x^{\mathrm{DFT}}) \qquad (30)$$

as already alluded to in the introduction. Prominent examples of these so called hybrid functionals are PBE0 [19–21] and B3LYP [22–24]. The factor α in front of the Hartree-Fock exact-exchange term is equivalent to a constant static screening function. Alternatively a more complex screening function can be chosen as in the screened-exchange (sX-LDA) approach [17,28,115,116], the Σ-GKS scheme [117] or the Heyd-Scuseria-Ernzerhof (HSE) functional [25–27]. An appealing feature of the hybrid functional approach is that it incorporates part of the derivative discontinuity of the exchange-correlation energy [17], because a quasiparticle equation (11) with a non-local potential is solved. For semiconductors and insulators this leads to a much improved description of band gaps [27,66,115,116,118–120]. From the point of perturbation theory this is again beneficial since the perturbation required by the GW (or eventually the true) self-energy is smaller. However, the dependence on universal (i.e. material independent) parameters questions the *ab initio* character of today's hybrid functionals.

While ample experience with hybrid functionals exists in the quantum chemistry community applications to solids are only slowly emerging and many issues remain open or controversial i.e. computational efficiency, basis sets, pseudopotentials or the choice of functional. In particular with regard to structural properties systematic studies are required. Conversely, GW quasiparticle energy calculations have traditionally fallen into the realm of condensed matter physics, but also here similar open questions remain (most of which have not been explicitly discussed in this article) including that of self-consistency. Again in a more pragmatic fashion the latter has recently been approached by mapping the G_0W_0 self-energy back onto a static, non-local potential. The eigenenergies and eigenfunctions of the new non-local, hermitian Hamiltonian then serve as input for the next G_0W_0 cycle until self-consistency is reached [46,121]. This approach shows promising success for different types of materials ranging from semiconductors, insulators and metals to transition metal oxides and f-electron systems [46,121,29,122].

Although the G_0W_0 approximation is currently the state of the art approach to calculate defect levels for solids from first principles it has so far only been applied in a few cases [123–128]. Ideally the GW calculations would encompass the determination of the defect structure, too, but so far GW total energy calculations, that would be required for this task, are still in their infancy. Meanwhile a combination of exact-exchange-based DFT functionals (for the structural properties) with quasiparticle energy calculations in the GW approach and the G_0W_0 approximation (for the spectral properties) offer the possibility to develop a better understanding of defect properties untainted by structural artefacts caused by the self-interaction or the band gap underestimation of Kohn-Sham. First G_0W_0 calculations for bulk semiconductors based on hybrid functionals appear to be promising [29–31], but more work along these lines is needed in the future.

[18] Some hybrid schemes introduce additional parameters for mixing different portions of the local-spin density (LSD) functional with GGA exchange and correlation in the E_{xc}^{DFT} term [21].

Acknowledgements We acknowledge stimulating discussions with Sixten Boeck, Martin Fuchs, Matthias Wahn, Hong Jiang and Christoph Freysoldt. This work was in part supported by the Volkswagen Stiftung/Germany, the DFG research group „nitride based nanostructures" and the EU's 6th Framework Programme through the NANOQUANTA (Contract No. NMP4-CT-2004-500198) Network of Excellence.

References

[1] L. Hedin, Phys. Rev. **139**, A796 (1965).
[2] W. G. Aulbur, L. Jönsson, and J. W. Wilkins, Solid State Phys. : Advances in Research and Applications **54**, 1 (2000).
[3] G. Onida, L. Reining, and A. Rubio, Rev. Mod. Phys. **74**, 601 (2002).
[4] T. Kotani, Phys. Rev. B **50**, 14816 (1994), *ibid.* **51**, 13903(E) (1995).
[5] T. Kotani, Phys. Rev. Lett. **74**, 2989 (1995).
[6] T. Kotani and H. Akai, Phys. Rev. B **54**, 16502 (1996).
[7] A. Görling, Phys. Rev. B **53**, 7024 (1996).
[8] M. Städele, J. A. Majewski, P. Vogl, and A. Görling, Phys. Rev. Lett. **79**, 2089 (1997).
[9] M. Städele, M. Moukara, J. A. Majewski, P. Vogl, and A. Görling, Phys. Rev. B **59**, 10031 (1999).
[10] W. G. Aulbur, M. Städele, and A. Görling, Phys. Rev. B **62**, 7121 (2000).
[11] A. Fleszar, Phys. Rev. B **64**, 245204 (2001).
[12] D. Gall, M. Städele, K. Järrendahl, I. Petrov, P. Desjardins, R. T. Haasch, T. Y. Lee, and J. E. Greene, Phys. Rev. B **63**, 125119 (2001).
[13] N. Fitzer, A. Kuligk, R. Redmer, M. Städele, S. M. Goodnick, and W. Schattke, Phys. Rev. B **67**, R201201 (2003).
[14] R. J. Magyar, A. Fleszar, and E. K. U. Gross, Phys. Rev. B **69**, 045111 (2004).
[15] A. Qteish, A. I. Al-Sharif, M. Fuchs, M. Scheffler, S. Boeck, and J. Neugebauer, Phys. Rev. B **72**, 155317 (2005).
[16] S. Kümmel and L. Kronik, Rev. Mod. Phys. (2007).
[17] A. Seidl, A. Görling, P. Vogl, J. A. Majewski, and M. Levy, Phys. Rev. B **53**, 3764 (1996).
[18] J. Perdew and A. Zunger, Phys. Rev. B **23**, 5048 (1981).
[19] J. P. Perdew, M. Ernzerhof, and K. Burke, J. Chem. Phys **105**, 9982 (1996).
[20] M. Ernzerhof and G. E. Scuseria, J. Chem. Phys **110**, 5029 (1999).
[21] C. Adamo and V. Barone, J. Chem. Phys **110**, 6158 (1999).
[22] A. D. Becke, J. Chem. Phys. **98**, 1372 (1993).
[23] A. D. Becke, J. Chem. Phys. **98**, 5648 (1993).

Copyright line will be provided by the publisher

[24] P. J. Stephens, F. J. Devlin, C. F. Chabalowski, and M. J. Frisch, J. Phys. Chem. **98**, 11623 (1994).
[25] J. Heyd, G. E. Scuseria, and M. Ernzerhof, J. Chem. Phys **118**, 8207 (2003).
[26] J. Heyd and G. E. Scuseria, J. Chem. Phys **120**, 7274 (2004).
[27] J. Heyd and G. E. Scuseria, J. Chem. Phys **121**, 1187 (2004).
[28] D. M. Bylander and L. Kleinman, Phys. Rev. B **41**, 7868 (1990).
[29] F. Bruneval, N. Vast, and L. Reining, Phys. Rev. B **74**, 045102 (2006).
[30] F. Fuchs, J. Furthmüller, F. Bechstedt, M. Shishkin, and G. Kresse, Phys. Rev. B **76**, 115109 (2007).
[31] Z. Zanolli, F. Fuchs, J. Furthmüller, U. von Barth, and F. Bechstedt, Phys. Rev. B **75**, 245121 (2007).
[32] P. Rinke, A. Qteish, J. Neugebauer, C. Freysoldt, and M. Scheffler, New J. Phys. **7**, 126 (2005).
[33] P. Rinke, A. Qteish, M. Winkelnkemper, D. Bimberg, J. Neugebauer, and M. Scheffler, Appl. Phys. Lett. **89**, 161919 (2006).
[34] A. Qteish, P. Rinke, J. Neugebauer, and M. Scheffler, Phys. Rev. B **74**, 245208 (2006).
[35] F. J. Himpsel, Adv. Physics **32**, 1 (1983).
[36] E. W. Plummer and W. Eberhardt, Adv. Chem. Phys. **49**, 533 (1982).
[37] L. Kevan (ed.), Angle-Resolved Photoemission (Elsevier, Amsterdam, 1992).
[38] V. Dose, Surface Science Reports **5**, 337 (1985).
[39] N. V. Smith, Rep. Prog. Phys. **51**, 1227 (1988).
[40] J. C. Fuggle and J. E. Inglesfield (eds.), Unoccupied Electronic States (Springer-Verlag, 1992).
[41] C. O. Almbladh and L. Hedin, in: Handbook on Synchroton Radiation, edited by E. E. Koch, (North Holland, 1983), pp. 607–904.
[42] W. Ku and A. G. Eguiluz, Phys. Rev. Lett. **89**, 126401 (2002).
[43] M. L. Tiago, S. Ismail-Beigi, and S. G. Louie, Phys. Rev. B **69**, 125212 (2003).
[44] K. Delaney, P. García-González, A. Rubio, P. Rinke, and R. W. Godby, Phys. Rev. Lett. **93**, 249701 (2004).
[45] N. E. Zein, S. Y. Savrasov, and G. Kotliar, Phys. Rev. Lett. **96**, 226403 (2006).
[46] M. van Schilfgaarde, T. Kotani, and S. Faleev, Phys. Rev. Lett. **96**, 226402 (2006).
[47] B. Holm and U. von Barth, Phys. Rev. B **57**, 2108 (1998).
[48] W. Luo, S. Ismail-Beigi, M. L. Cohen, and S. G. Louie, Phys. Rev. B **66**, 195215 (2002).
[49] A. Fleszar and W. Hanke, Phys. Rev. B **71**, 045207 (2005).
[50] M. Marsili, O. Pulci, F. Bechstedt, and R. Del Sole, Phys. Rev. B **72**, 115415 (2005).
[51] R. Del Sole, L. Reining, and R. W. Godby, Phys. Rev. B **49**, 8024 (1994).
[52] F. Bruneval, F. Sottile, V. Olevano, R. Del Sole, and L. Reining, Phys. Rev. Lett. **94**, 186402 (2005).
[53] A. J. Morris, M. Stankovski, K. T. Delaney, P. Rinke, P. García-González, and R. W. Godby, Phys. Rev. B **76**, 155106 (2007).
[54] For the upper valence and conduction bands of standard semiconductors numerical investigations indicate that this approximation is well justified [2, 129], but it breaks down for certain surface [130–133] and cluster states [134, 135].
[55] P. Hohenberg and W. Kohn, Phys. Rev. **136**, B864 (1964).
[56] W. Kohn and K. J. Sham, Phys. Rev. **140**, A1133 (1965).
[57] A. Görling and M. LevyPhys. Rev. A, **50**, 196 (1994); *ibid*. Phys. Rev. B, **47**, 13105 (1993).
[58] O. Gunnarsson and B. I. Lundqvist, Phys. Rev. B **13**, 4274 (1976).
[59] W. Nelson, P. Bokes, P. Rinke, and R. Godby, Phys. Rev. A **75**, 032505 (2007).
[60] M. E. Casida, Phys. Rev. A **51**, 2005 (1995).
[61] R. Grabo, T. Kreibich, S. Kurth, and E. K. U. Gross, in Strong Coulomb Correlations in Electronic Structure Calculations: Beyond the Local Density Approximation edited by V. I. Anisimov (Gordon and Breach, New York, 2000),), pp. 203–311.
[62] Y. M. Niquet, M. Fuchs, and X. Gonze, J. Chem. Phys. **118**, 9504 (2003).
[63] E. Engel, in A Primer in Density-Functional Theory edited by C. Fiolhais, F. Nogueira and M. Marques (Springer, Berlin, 2003),), pp. 56–122.
[64] S. Ivanov and M. Levy, J. Chem. Phys. **119**, 7087 (2003).
[65] S. Sharma, J. K. Dewhurst, and C. Ambrosch-Draxl, Phys. Rev. Lett. **95**, 136402 (2005).
[66] M. Grüning, A. Marini, and A. Rubio, Phys. Rev. B **R74**, 161103 (2006).
[67] D. Ceperley and B. Alder, Phys. Rev. Lett. **45**, 566 (1980).
[68] D. Vogel, P. Krüger, and J. Pollmann, Phys. Rev. B **54**, 5495 (1996).
[69] Hong Jiang, private communications.
[70] C. E. Moore, Atomic Energy Levels, Natl. Bur. Stand (U.S.) Circ. No. 467 (U.S. GPO, Washington, DC, 1949), Vol. I; ibid. (U.S. GPO, Washington, DC, 1952), Vol. II; ibid. (U.S. GPO, Washington, DC, 1958), Vol. III.).
[71] K. Aashamar, T. M. Luke, and J. D. Talman, Phys. Rev. A **19**, 6 (1979).
[72] D. Vogel, P. Krüger, and J. Pollmann, Phys. Rev. B **52**, R14316 (1995).
[73] D. Vogel, P. Krüger, and J. Pollmann, Phys. Rev. B **55**, 12836 (1997).
[74] C. Almbladh and U. von Barth, Phys. Rev. B **31**, 3231 (1985).
[75] M. Levy, J. P. Perdew, and V. Sahni, Phys. Rev. A **30**, 2745 (1984).
[76] M. E. Casida, Phys. Rev. B **59**, 4694 (1999).
[77] J. Perdew and M. Levy, Phys. Rev. Lett. **51**, 1884 (1983).
[78] L. Sham and M. Schlüter, Phys. Rev. Lett. **51**, 1888 (1983).
[79] R. W. Godby, M. Schlüter, and L. J. Sham, Phys. Rev. Lett. **56**, 2415 (1986).
[80] J. B. Krieger, Y. Li, and G. J. Iafrate, Phys. Rev. B **45**, 101 (1992).
[81] M. Grüning, A. Marini, and A. Rubio, J. Chem. Phys **124**, 154108 (2006).
[82] K. Schönhammer and O. Gunnarsson, Phys. Rev. Lett. **56**, 1968 (1986).
[83] K. Schönhammer and O. Gunnarsson, J. Phys. C: Solid State Phys. **20**, 3675 (1987).

Copyright line will be provided by the publisher

[84] R. W. Godby, M. Schlüter, and L. J. Sham, Phys. Rev. B **37**, 10159 (1988).
[85] Numerical Data and Functional Relationships in Science and Technology, edited by O. Madelung New Series, Group III, Vols. 22, Pt. a, (Springer, Berlin, 1982)).
[86] O. Madelung and Landolt-Börnstein, Semiconductors. Intrinsic Properties of Group IV Elements and III-V, II-VI and I-VII Compounds, New Series, Group III, Vols. 22, Pt. a (Springer, Berlin, 1982)).
[87] D. R. T. Zahn, G. Kudlek, U. Rossow, A. Hoffmann, I. Broser, and W. Richter, Adv. Mater. Opt. Electron. **3**, 11 (1994).
[88] G. Ramírez-Flores, H. Navarro-Contreras, A. Lastras-Martínez, R. C. Powell, and J. E. Greene, Phys. Rev. B **50**, 8433 (1994).
[89] O. Zakharov, A. Rubio, X. Blase, M. L. Cohen, and S. G. Louie, Phys. Rev. B **50**, 10780 (1994).
[90] A. Rubio, J. L. Corkill, M. L. Cohen, E. L. Shirley, and S. G. Louie, Phys. Rev. B **48**, 11810 (1993).
[91] M. Rohlfing, P. Krüger, and J. Pollmann, Phys. Rev. Lett. **75**, 3489 (1995).
[92] M. Rohlfing, P. Krüger, and J. Pollmann, Phys. Rev. B **57**, 6485 (1998).
[93] M. Usuda, N. Hamada, T. Kotani, and M. van Schilfgaarde, Phys. Rev. B **66**, 125101 (2002).
[94] T. Kotani and M. van Schilfgaarde, Solid State Commun. **121**, 461 (2002).
[95] M. Oshikiri and F. Aryasetiawan, Phys. Rev. B **60**, 10754 (1999).
[96] M. Oshikiri and F. Aryasetiawan, J. Phys. Soc. Jap. **69**, 2113 (2000).
[97] M. Moukara, M. Städele, J. A. Majewski, P. Vogl, and A. Görling, J. Phys. Condens. Matter **12**, 6783 (2000).
[98] S. G. Louie, S. Froyen, and M. L. Cohen, Phys. Rev. B **26**, 1738 (1982).
[99] M. Usuda, N. Hamada, K. Shiraishi, and A. Oshiyama, Jpn. J. Appl. Phys. **43**, L407 (2004).
[100] F. Bechstedt and J. Furthmüller, J. Cryst. Growth **246**, 315 (2002).
[101] J. Furthmüller, P. H. Hahn, F. Fuchs, and F. Bechstedt, Phys. Rev. B **72**, 205106 (2005).
[102] V. Y. Davydov, A. A. Klochikhin, R. P. Seisyan, V. V. Emtsev, S. Ivanov, F. Bechstedt, J. Furthmüller, H. Harima, A. V. Mudryi, J. Aderhold, O. Semchinova, and J. Graul, phys. stat. sol. (b) **229**, R1 (2002).
[103] J. Wu, W. Walukiewicz, K. M. Yu, J. W. Ager III, E. E. Haller, H. Lu, W. Schaff, Y. Saiton, and Y. Nanishi, Appl. Phys. Lett. **80**, 3967 (2002).
[104] Y. Nanishi, Y. Saito, and T. Yamaguchi, Japan. J. Appl. Phys. **42**, 2549 (2003).
[105] H. A. Al-Brithen, A. R. Smith, and D. Gall, Phys. Rev. B **70**, 045303 (2004).
[106] R. Weidemann, H. E. Gumlich, M. Kupsch, H. U. Middelmann, and U. Becker, Phys. Rev. B **45**, 1172 (1992).
[107] Semiconductors: Technology of III-V, II-VI and Non-Tetrahedrally Bonded Compounds edited by O. Madelung, Landolt-Börnstein, New Series, Group III, Vol. 17, Pt. d (Springer, Berlin, 1982)).
[108] S. A. Ding, G. Neuhold, J. H. Weaver, P. Häberle, K. Horn, O. Brandt, H. Yang, and K. Ploog, J. Vac. Sci. Technol. A **14**, 819 (1996).
[109] L. Ley, R. A. Pollak, F. R. McFeely, S. P. Kowalczyk, and D. A. Shirley, Phys. Rev. B **9**, 600 (1974).
[110] M. Rohlfing, P. Krüger, and J. Pollmann, Phys. Rev. B **56**, R7065 (1997).
[111] T. Miyake, P. Zhang, M. L. Cohen, and S. G. Louie, Phys. Rev. B **74**, 245213 (2006).
[112] M. M. Rieger, L. Steinbeck, I. White, H. Rojas, and R. Godby, Comput. Phys. Commun. **117**, 211 (1999).
[113] L. Steinbeck, A. Rubio, L. Reining, M. Torrent, I. White, and R. Godby, Comput. Phys. Commun. **125**, 105 (2000).
[114] C. Freysoldt, P. Eggert, P. Rinke, A. Schindlmayr, R. W. Godby, and M. Scheffler, Comput. Phys. Commun. **176**, 1 (2007).
[115] R. Asahi, W. Mannstadt, and A. J. Freeman, Phys. Rev. B **59**, 7486 (1999).
[116] S. H. Rhim, M. Kim, A. J. Freeman, and R. Asahi, Phys. Rev. B **71**, 045202 (2005).
[117] P. Sánchez-Friera and R. W. Godby, Phys. Rev. Lett. **85**, 5611 (2000).
[118] J. Muscat, A. Wander, and N. M. Harrison, Chem. Phys. Lett. **342**, 397 (2001).
[119] F. Cora, M. Alfredsson, G. Mallia, D. S. Middlemiss, W. C. Mackrodt, R. Dovesi and R. Orlando in *Principles and applications of density functional theory in inorganic chemistry II* edited by N. Kaltsoyannis and J. E. McGrady (Springer, Berlin, 2004) p171–232.
[120] J. Paier, M. Marsman, K. Hummer, G. Kresse, I. C. Gerber, and J. G. Ángyán, J. Chem. Phys. **124**, 154709 (2006).
[121] S. V. Faleev, M. van Schilfgaarde, and T. Kotani, Phys. Rev. Lett. **93**, 126406 (2004).
[122] F. Bruneval, N. Vast, L. Reining, M. Izquierdo, F. Sirotti, and N. Barrett, Phys. Rev. Lett. **97**, 267601 (2006).
[123] B. Králik, E. K. Chang, and S. G. Louie, Phys. Rev. B **57**, 7027 (1998).
[124] M. P. Surh, H. Chacham, and S. G. Louie, Phys. Rev. B **51**, 7464 (1995).
[125] M. L. Tiago and J. R. Chelikowsky, Phys. Rev. B **73**, 205334 (2006).
[126] M. Hedström, A. Schindlmayr, and M. Scheffler, phys. stat. sol. b **234**, 346 (2002).
[127] M. Hedström, A. Schindlmayr, G. Schwarz, and M. Scheffler, Phys. Rev. Lett. **97**, 226401 (2006).
[128] J. Weber, A. Janotti, P. Rinke, and C. G. Van de Walle, Appl. Phys. Lett. **91**, 142101 (2007).
[129] F. Aryasetiawan and O. Gunnarsson, Rep. Prog. Phys. **61**, 237 (1998).
[130] I. D. White, R. W. Godby, M. M. Rieger, and R. J. Needs, Phys. Rev. Lett. **80**, 4265 (1997).
[131] M. Rohlfing, N. P. Wang, P. Krüger, and J. Pollmann, Phys. Rev. Lett. **91**, 256802 (2003).
[132] G. Fratesi, G. P. Brivio, P. Rinke, and R. Godby, Phys. Rev. B **68**, 195404 (2003).
[133] G. Fratesi, G. P. Brivio, and L. G. Molinari, Phys. Rev. B **69**, 245113 (2004).
[134] O. Pulci, L. Reining, G. Onida, R. D. Sole, and F. Bechstedt, Comp. Mater. Sci. **20**, 300 (2001).
[135] P. Rinke, K. Delaney, P. García-González, and R. W. Godby, Phys. Rev. A **70**, 063201 (2004).

Copyright line will be provided by the publisher